Mol. Cells *36*, 163-168, August 31, 2013
DOI/10.1007/s10059-013-0147-1
eISSN: 0219-1032

Molecules and Cells
http://molcells.org
Established in 1990

Tbc1d15-17 Regulates Synaptic Development at the *Drosophila* Neuromuscular Junction

Min-Jung Lee, Sooyeon Jang[1], Minyeop Nahm, Jin-Ho Yoon[1,*], and Seungbok Lee*

Members of the Tre-2/Bub2/Cdc16 (TBC) family of proteins are believed to function as GTPase-activating proteins (GAPs) for Rab GTPases, which play pivotal roles in intracellular membrane trafficking. Although membrane trafficking is fundamental to neuronal morphogenesis and function, the roles of TBC-family Rab GAPs have been poorly characterized in the nervous system. In this paper, we provide genetic evidence that Tbc1d15-17, the *Drosophila* homolog of mammalian Rab7-GAP TBC1d15, is required for normal presynaptic growth and postsynaptic organization at the neuromuscular junction (NMJ). A loss-of-function mutation in *tbc1d15-17* or its presynaptic knockdown leads to an increase in synaptic bouton number and NMJ length. *tbc1d15-17* mutants are also defective in the distribution of the postsynaptic scaffold Discs-large (Dlg) and in the level of the postsynaptic glutamate subunit GluRIIA. These postsynaptic phenotypes are recapitulated by postsynaptic knockdown of Tbc1d15-17. We also show that presynaptic overexpression of a constitutively active Rab7 mutant in a wild-type background causes a synaptic overgrowth phenotype resembling that of *tbc1d15-17* mutants, while a dominant-negative form of Rab7 has the opposite effect. Together, our findings establish a novel role for Tbc1d15-17 and its potential substrate Rab7 in regulating synaptic development.

INTRODUCTION

Rab GTPases constitute the largest subgroup of the Ras GTPase superfamily and play key roles in controlling membrane trafficking (Stenmark, 2009). Like other Ras-superfamily members, they serve as molecular switches that cycle between an active, GTP-bound state and an inactive, GDP-bound state. Activated, GTP-bound Rabs perform their biological functions by recruiting and activating specific effector molecules that are involved in vesicle budding, motility, tethering, and fusion (Stenmark, 2009). Interconversion between these alternate states is primarily regulated by guanine nucleotide exchange factors (GEFs) and by GTPase-activating proteins (GAPs). GEFs facilitate the release of GDP from Rab GTPases, thereby promoting the exchange of GDP for GTP, while GAPs enhance the intrinsic GTPase activity of Rab proteins, converting GTP-bound Rabs to the GDP-bound state (Barr and Lambright, 2010). Except Rab3GAP, all proteins that have been proven or are expected to be Rab GAPs have a Tre-2, Bub2, and Cdc16 (TBC) domain, which has a catalytic 'arginine finger' analogous to those of Ras and Rho family GAPs (Albert et al., 1999; Barr and Lambright, 2010).

It has recently emerged that Rab GTPases and their regulators play essential roles in the regulation of neuronal development. Protrudin mediates nerve growth factor (NGF)-induced neurite formation *via* its antagonistic action on Rab11 (Shirane and Nakayama, 2006). The mammalian homolog of *Drosophila* Lethal giant larvae (Lgl1) is shown to control axonal outgrowth by activating Rab10 (Wang et al., 2011a). In addition, *Drosophila* Rab11 is required for normal synaptic morphogenesis at the neuromuscular junction (NMJ) (Khodosh et al., 2006). Finally, mammalian Rab17 is shown to play an essential role in the regulation of dendritic morphogenesis and postsynaptic development (Mori et al., 2012). Although these studies suggest the importance of Rab-dependent membrane trafficking in multiple aspects of neuronal morphogenesis, little is known about the roles of Rab-specific GEFs and GAPs in the developing nervous system.

Recent studies in mammals suggest that Tbc1d15 has a GAP activity selective for Rab7 (Peralta et al., 2010), which is a key regulator of endosomal maturation and endo-lysosomal trafficking (Wang et al., 2011b). Here, we describe a synaptic role of Tbc1d15-17, the single *Drosophila* ortholog of mammalian TBC domain-containing proteins Tbc1d15 and Tbc1d17. Our genetic data demonstrate that Tbc1d15-17 is required presynaptically and postsynaptically for normal presynaptic growth and postsynaptic organization, respectively, at the neuromuscular junction (NMJ). Consistent with expectation for Rab7 GAP, Tbc1d15-17 is targeted to Rab7-positive intracellular structures in cultured cells. Moreover, neuronal expression of a constitutively-active form of Rab7 produces an NMJ overgrowth phenotype resembling that of *tbc1d15-17* mutants. Together, our data establish a novel role for Tbc1d15-17 and Rab7 in regulating synapse development.

Department of Cell and Developmental Biology, Dental Research Institute, School of Dentistry, Seoul National University, Seoul 110-749, Korea, [1]School of Biological Sciences and Chemistry, Sungshin Women's University, Seoul 136-742, Korea
*Correspondence: jhoyoon@sungshin.ac.kr (JHY); seunglee@snu.ac.kr (SL)

Received May 13, 2013; accepted May 23, 2013; published online June 27, 2013

Keywords: *Drosophila* NMJ, postsynaptic organization, synaptic growth, Tbc1d15-17

Springer

MATERIALS AND METHODS

Drosophila stocks

Flies were maintained on standard fly food at 25°C. w^{1118} was used as the wild-type strain in this study. A transposable P-element insertion line of *tbc1d15-17* (*tbc1d15-17*^{d05023}) and transgenic lines carrying *UAS-tbc1d15-17*^{RNAi}, *UAS-YFP-rab7Q67L*, or *UAS-YFP-rab7T22N* were obtained from the Bloomington Stock Center (USA). UAS transgenes were driven by *C155-GAL4* (Lin and Goodman, 1994), *BG57-GAL4* (Budnik et al., 1996), and *da-GAL4* (Wodarz et al., 1995).

Molecular biology

A full-length cDNA clone encoding Tbc1d15-17 was obtained from the *Drosophila* Genomics Resource Center (Clone ID: LD27216; USA). For expression in S2 cells, the entire *tbc1d15-17* open reading frame was PCR amplified and subcloned into *pUAST-HA,* a derivative of the GAL4-based expression vector pUAST (Brand and Perrimon, 1993), to produce *pUAST-HA-tbc1d15-17*.

Cell transfection

Drosophila Schneider S2R+ cells were cultured in Schneider's medium (Invitrogen, USA) containing 10% heat-inactivated fetal bovine serum (FBS) at 25°C and were transiently transfected with *pUAST-HA-tbc1d15-17* and an actin5C promoter-GAL4 construct along with *pAc-rab5-GFP* or *pAc-rab7-GFP*, in six-well plates using Cellfectin (Invitrogen, USA), according to the manufacturer's instructions.

Reverse transcription (RT)-PCR

Levels of *tbc1d15-17*, *CG11617,* and *rp49* mRNAs in *tbc1d15-17*^{d05023} or larvae expressing *UAS-tbc1d15-17*^{RNAi} driven by *da-GAL4* were determined by RT-PCR. Briefly, total RNA was extracted from third-instar larvae using TRIzol reagent (Invitrogen, USA) and reverse-transcribed into cDNA with an oligo-dT primer and the SuperScript II RT kit (Invitrogen, USA), as previously described (Nahm et al., 2010). The resulting cDNA was amplified by PCR using the following primers: *tbc1d15-17*, 5′-TGTT CCTCAAACGGACAGTCTCGT-3′ and 5′-AAATGGGCG CAAGCAGATCGGACA-3′; *CG11617*, 5′-TATGCGAGATAGT TCCACGGCAAA-3′ and 5′-TTGAAGAAAATCATGTAACGA GTG-3′; and *rp49*, 5′-CACCAGTCGGATCGATATGC-3′ and 5′-CACG TTGTGCACCAGGAACT-3′.

Immunohistochemistry and morphological quantification of NMJs

Wandering third-instar larvae were dissected in Ca^{2+}-free HL3 saline (70 mM NaCl, 5 mM KCl, 20 mM $MgCl_2$, 10 mM $NaHCO_3$, 5 mM trehalose, 115 mM sucrose, 5 mM HEPES pH 7.2) (Stewart et al., 1994). Dissected larval fillets were fixed in either 4% formaldehyde in PBS for 20 min or Bouin's fixative for 10 min at room temperature, washed with PBS containing 0.1% Triton X-100 (PBT) for 10 min three times, and incubated with primary antibodies for 2 h at room temperature or overnight at 4°C. The samples were then incubated with fluorescence-conjugated secondary antibodies for 1 h at room temperature. The following antibodies were used in this study: anti-Dlg (4F3, DSHB; 1:500), anti-GluRIIA (8B4D2, DSHB; 1:10), anti-Csp (1G12, DSHB; 1:100), anti-Bruchpilot (NC82, DSHB; 1:10) and

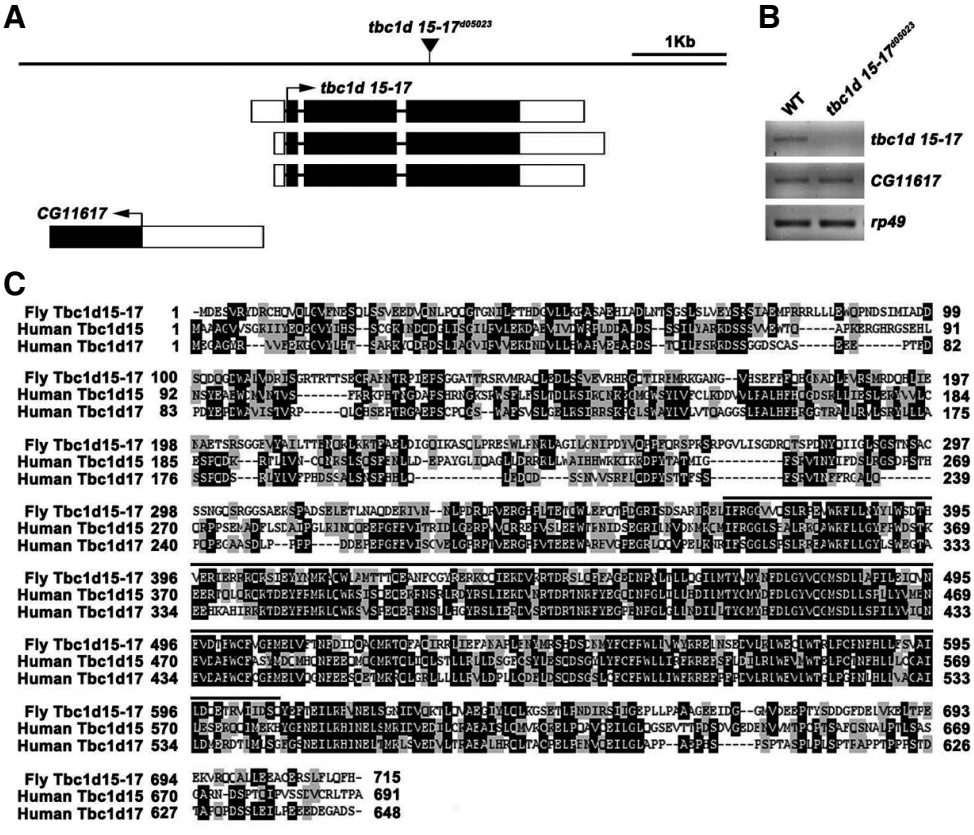

Fig. 1. *tbc1d15* locus and mutant. (A) Genomic organization of the *tbc1d15-17* locus. Exons are designated by boxes; introns by horizontal lines. Black and white boxes indicate translated and untranslated regions, respectively. The position of the P-element *tbc1d15-17*^{d05023} is indicated by an inverted triangle. (B) RT-PCR analysis of wild-type (WT) and *tbc1d15-17*^{d05023} third instar larvae using primers specific for *tbc1d15-17*, *CG11617*, and *rp49*. (C) Sequence alignment of *Drosophila* Tbc1d15-17 (GenBank accession number AAK93170) and human Tbc1d15 (AAH28352) and Tbc1d17 (AAH03516). Identical residues are indicated by white letters on black background; similar residues by black letters on gray background. The TBC (Tre-2/Bub2/Cdc16) domain is overlined.

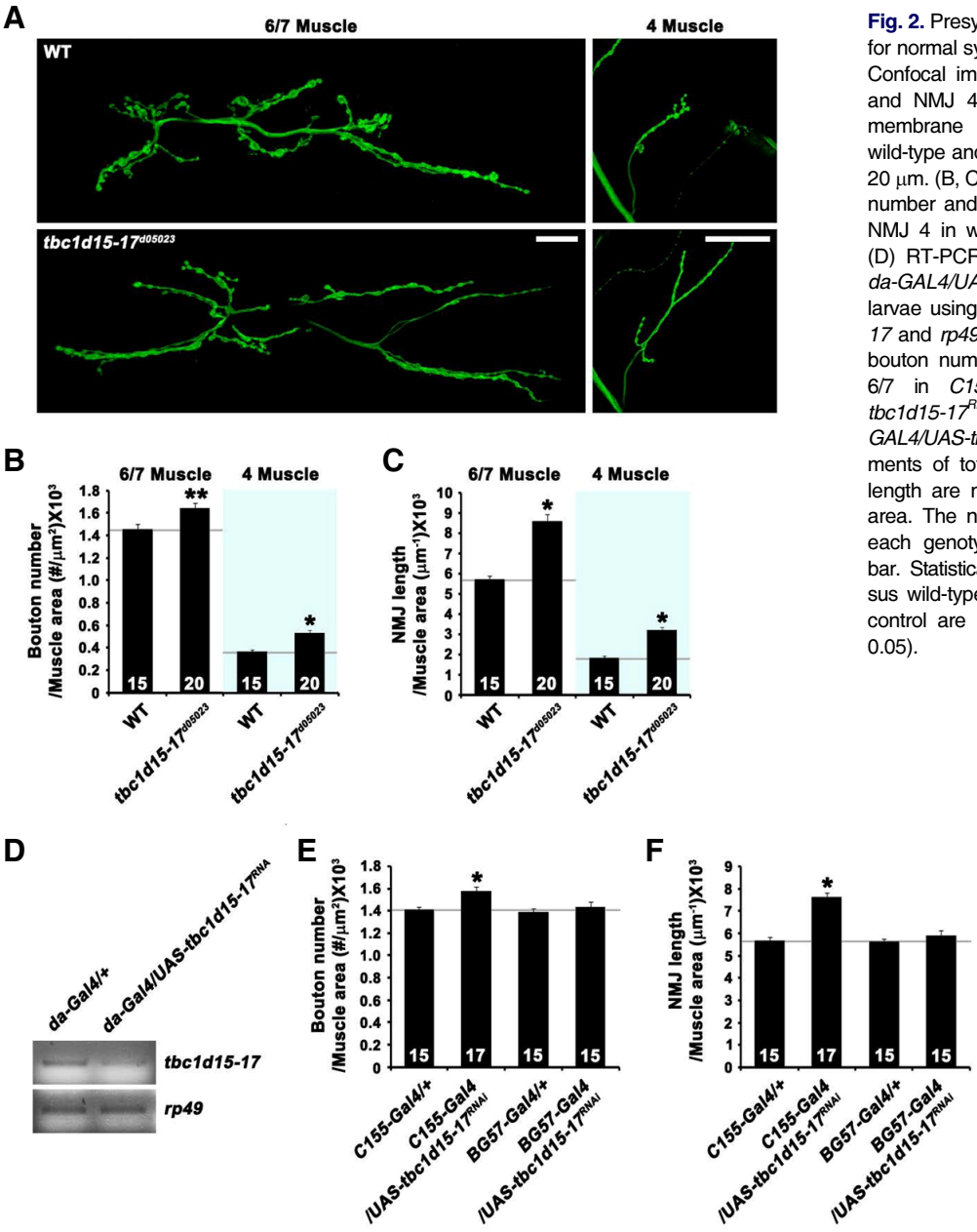

Fig. 2. Presynaptic Tbc1d15-17 is required for normal synaptic growth at the NMJ. (A) Confocal images of third instar NMJ 6/7 and NMJ 4 stained for the presynaptic membrane marker HRP are shown for wild-type and *tbc1d15-17*^{d05023}. Scale bars, 20 μm. (B, C) Quantification of total bouton number and NMJ length at NMJ 6/7 and NMJ 4 in wild-type and *tbc1d15-17*^{d05023}. (D) RT-PCR analysis of *da-GAL4/+* and *da-GAL4/UAS-tbc1d15-17*^{RNAi} third-instar larvae using primers specific for *tbc1d15-17* and *rp49*. (E, F) Quantification of total bouton number and NMJ length at NMJ 6/7 in *C155-GAL4/+*, *C155-GAL4/UAS-tbc1d15-17*^{RNAi}, *BG57-GAL4/+*, and *BG57-GAL4/UAS-tbc1d15-17*^{RNAi} larvae. Measurements of total bouton number and NMJ length are normalized to muscle surface area. The number of NMJs analyzed for each genotype is indicated inside each bar. Statistically significant differences versus wild-type or the corresponding GAL4 control are indicated (*$P < 0.001$; **$P < 0.05$).

FITC conjugated anti-HRP and FITC- or Cy3-conjugated secondary antibodies (Jackson Immuno Labs, USA; 1:200).

Images were acquired with a Zeiss LSM 700 or Olympus FV300 laser-scanning confocal microscope. Quantification of NMJ morphology and muscle surface area was performed at both muscles 6 and 7 and muscle 4 in abdominal segment 2, as described previously (Nahm et al., 2010). For quantification of GluRIIA levels, the fluorescence intensities of GluRIIA were measured using the FLOUVIEW software and then normalized to HRP intensities.

RESULTS AND DISCUSSION

Tbc1d15-17 is required presynaptically for normal synaptic growth at the *Drosophila* larval NMJs

The *Drosophila* genome contains at least 26 genes encoding TBC domain-containing proteins (Laflamme et al., 2012). As an attempt to study the synaptic role of these potential Rab GAPs, we performed an anatomical genetic screen for their P-element mutations that affect NMJ morphology. For this screen, we immunostained third instar larval fillets of homozygous mutants with an antibody against the axonal membrane protein HRP (Jan and Jan, 1982) and inspected their NMJs under fluorescence microscopy. To this end, we recovered a mutant allele of *tbc1d15-17* (*tbc1d15-17*^{d05023}) in which a P-element was in-

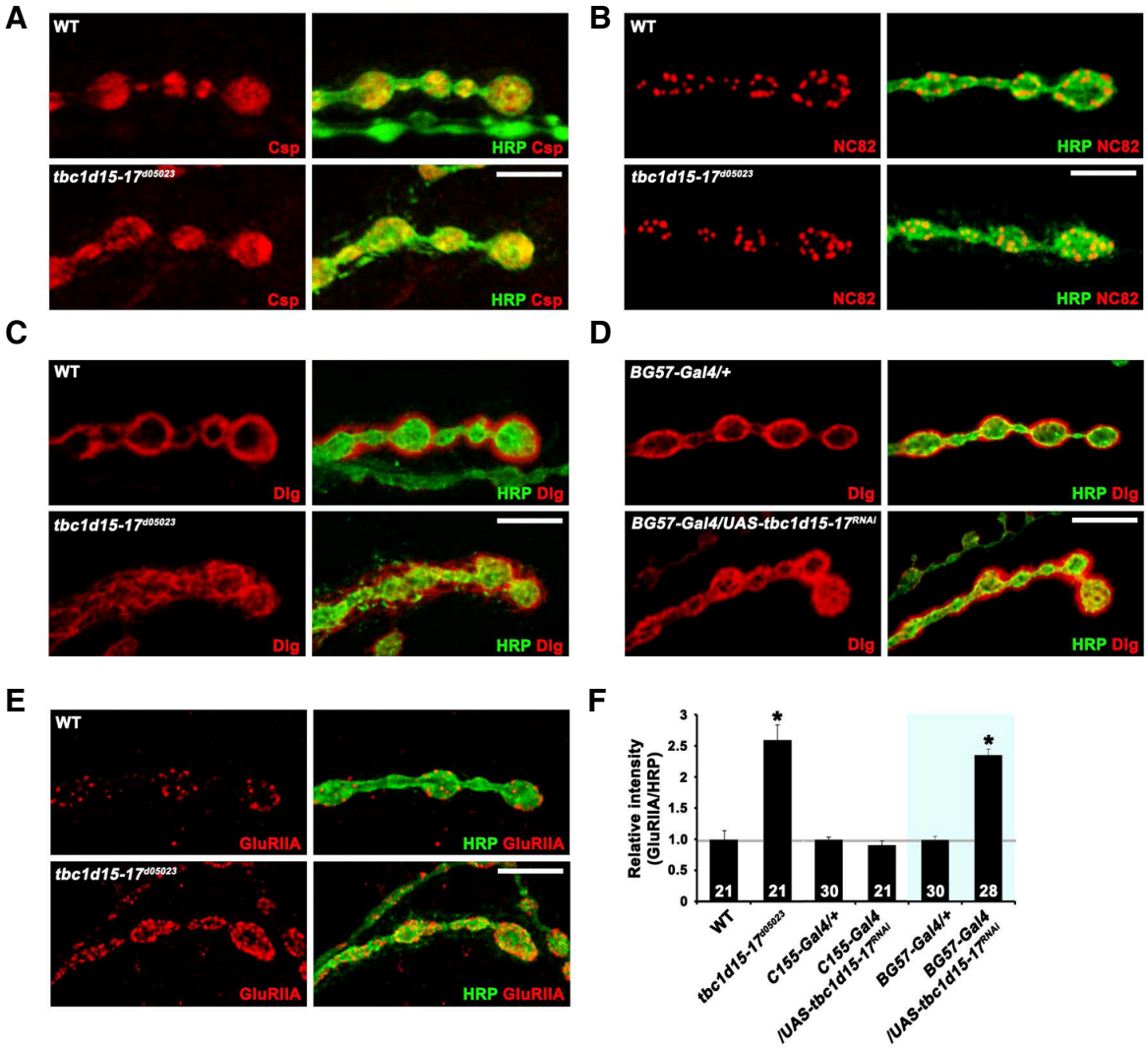

Fig. 3. Distribution of Dlg and synaptic levels of GluRIIA are altered in *tbc1d15-17* mutants. (A-E) Single confocal slices of NMJ 6/7 doubly stained with anti-HRP and anti-Csp (A), anti-NC82 (B), anti-Dlg (C, D), or anti-GluRIIA (E) antibodies in the indicated genotypes. Note that Dlg distribution and synaptic GluRIIA level are defective in *tbc1d15-17*^{d05023} (C) and *BG57-GAL4/UAS-tbc1d15-17*^{RNAi} (D) larvae. (E) Levels of synaptic GluRIIA are increased in *tbc1d15-17*^{d05023} mutants compared with wild-type larvae. (F) Quantification of GluRIIA to HRP level ratio in the indicated genotypes. Note that levels of GluRIIA are significantly increased in *BG57-GAL4/UAS-tbc1d15-17*^{RNAi} compared with the *BG57-GAL4/+* control (*$P < 0.001$). Scale bars, 20 μm.

serted within its fourth exon (Fig. 1A). RT-PCR analysis revealed that expression of the *tbc1d15-17* transcript was largely abolished in larvae homozygous for *tbc1d15-17*^{d05023}, while the adjacent gene (*CG11617*) was expressed at wild-type levels (Fig. 1B). The predicted Tbc1d15-17 protein showed the strongest homology to Tbc1d15 and Tbc1d17 among mammalian TBC proteins (overall 30% identity and 63% and 61% similarity to human Tbc1d15 and Tbc1d17, respectively; Fig. 1C).

Initial observation of NMJ morphology revealed a phenotype of synaptic overgrowth in *tbc1d15-17*^{d05023} mutant larvae (Fig. 2A). To quantify this phenotype, we measured total bouton number and NMJ length at NMJ 6/7 and NMJ 4. Compared with wild-type controls (w^{1118}), total bouton number normalized to muscle surface area was increased by 14% at NMJ 6/7 in homozygous *tbc1d15-17*^{d05023} mutants (wild-type, $1.44 \pm 0.03 \times 10^{-3}$ μm^{-2}; *tbc1d15-17*^{d05023}, $1.64 \pm 0.04 \times 10^{-3}$ μm^{-2}; $P < 0.05$; Fig. 2B) and by 47% at NMJ 4 (wild-type, $0.36 \pm 0.01 \times 10^{-3}$ μm^{-2}; *tbc1d15-17*^{d05023}, $0.53 \pm 0.02 \times 10^{-3}$ μm^{-2}; $P < 0.001$; Fig. 2B). In addition, NMJ length normalized to muscle surface area was increased by 50% at NMJ 6/7 in *tbc1d15-17*^{d05023} compared with wild-type (wild-type, 5.74 ± 0.14 μm$^{-1} \times 10^{-3}$; *tbc1d15-17*^{d05023}, 8.6 ± 0.32 μm$^{-1} \times 10^{-3}$; $P < 0.001$; Fig. 2C). At NMJ 4, the same parameter of synaptic overgrowth was increased by 77% in the mutant (wild-type, 1.82 ± 0.1 μm$^{-1} \times 10^{-3}$; *tbc1d15-17*^{d05023}, 3.23 ± 0.09 μm$^{-1} \times 10^{-3}$; $P < 0.001$; Fig. 2C).

To assess whether *tbc1d15-17* is required in presynaptic motor neurons or postsynaptic muscles for normal synaptic growth, we employed a transgenic RNA interference (RNAi) technique to deplete Tbc1d15-17 protein in a tissue-specific manner. We first demonstrated that we could significantly knockdown

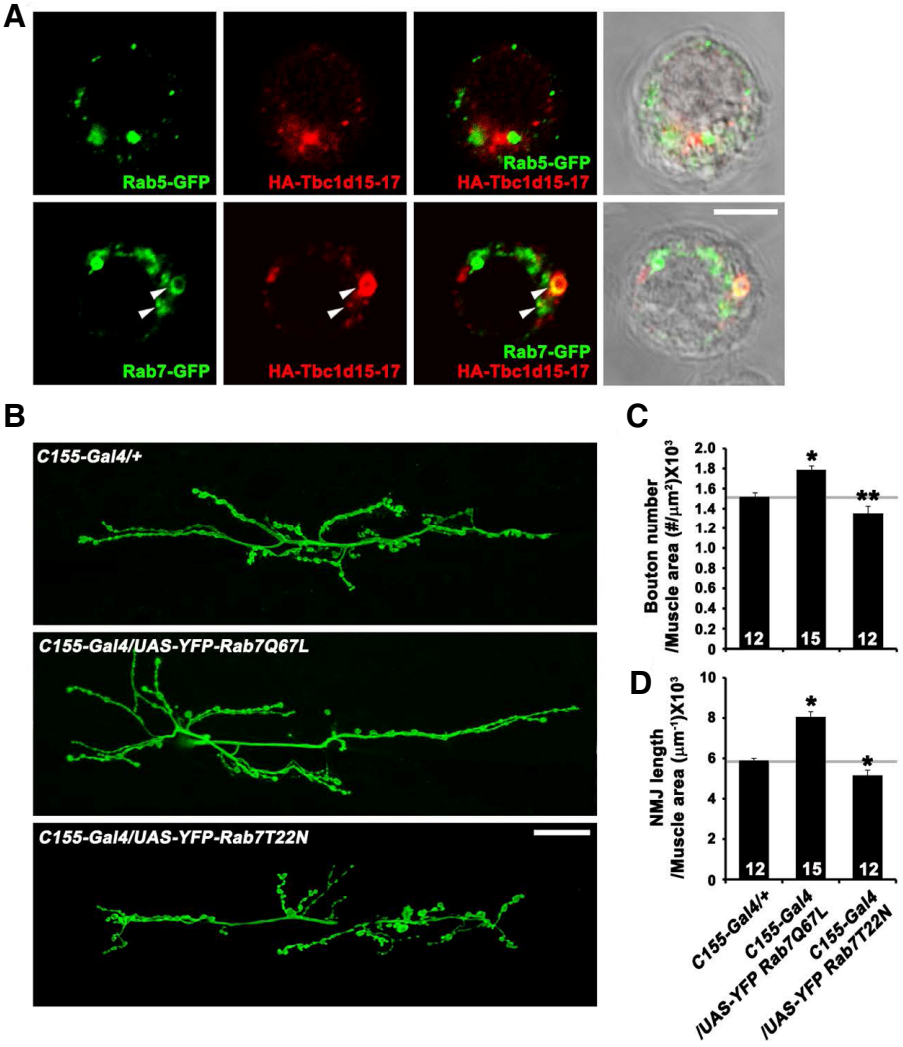

Fig. 4. (A) Confocal images of S2 cells overexpressing both HA-Tbc1d15-17 and GFP-Rab5 or GFP-Rab7 stained with anti-GFP and anti-HA antibodies. Some vesicular structures are labeled for both Tbc1d15-17 and Rab7 (arrows). (B-D) Presynaptic Rab7 regulates synaptic growth at the NMJ. (B) Confocal images of NMJ 6/7 labeled with anti-HRP in *C155-GAL4/+*, *C155-GAL4/UAS-YFP-Rab7Q67L*, and *C155-GAL4/UAS-YFP-Rab7T22N* third instar larvae. (C, D) Quantification of bouton number (C) and NMJ length (D) at NMJ 6/7. *$P < 0.001$. Scale bars, 20 μm.

tbc1d15-17 by expressing *UAS-tbc1d15-17^{RNAi}* with the ubiquitous *da-GAL4* driver (Fig. 2D). When the *UAS-tbc1d15-17^{RNAi}* transgene was expressed presynaptically using the pan-neuronal *C155-GAL4* driver, total bouton numbers and NMJ length were increased by 10% and 30%, respectively (Figs. 2E and 2F). However, *UAS-tbc1d15-17^{RNAi}* expression using the muscle-specific *BG57-GAL4* driver did not affect synaptic morphology (Figs. 2E and 2F). These data suggest that Tbc1d15-17 acts presynaptically to restrain synaptic growth.

The abundance or distribution of postsynaptic markers GluRIIA and Dlg are altered in *tbc1d15-17* mutants

We further examined potential defects in synaptic organization of *tbc1d15-17* mutant NMJs using various synaptic markers. We observed no defects in the levels and distribution of the presynaptic vesicle marker Csp and the active zone antigen Bruchpilot (NC82) in *tbc1d15-17^{d05023}* (Figs. 3A and 3B). In contrast, the distribution of Discs-large (Dlg), a postsynaptic subsynaptic reticulum (SSR) marker, was defective in the mutant. In wild-type, Dlg immunoreactivity was homogeneously detected in a halo-like structure surrounding type I boutons (Fig. 3C). In the *tbc1d15-17* mutants, Dlg immunoreactivity was not concentrated in a halo-like postsynaptic structure, but instead displayed a disorganized, honeycomb-like pattern (Fig. 3C). A similar phenotype was observed in larvae expressing *UAS-tbc1d15-17^{RNAi}* under the control of *BG57-GAL4* (Fig. 3D), suggesting a postsynaptic requirement for Tbc1d15-17. Another important postsynaptic protein at the *Drosophila* NMJ is the glutamate receptor (GluR). We used an antibody against the GluRIIA subunit to assess receptor clustering in *tbc1d15-17^{d05023}* mutants. Levels of synaptic GluRIIA were increased by 200% in *tbc1d15-17^{d05023}* compared with wild-type larvae ($P < 0.001$; Figs. 3E and 3F). Postsynaptic, but not presynaptic, expression of *UAS-tbc1d15-17^{RNAi}* also caused the same phenotype (Fig. 3F), suggesting that Tbc1d15-17 is required postsynaptically for proper postsynaptic organization.

rab7 gain-of-function mimics *tbc1d15-17* loss- of- function at the NMJ

Because Tbc1d15, a mammalian homolog of *Drosophila* Tbc1d15-17, is known to act as a Rab7-specific GAP (Peralta et al., 2010), we tested whether Tbc1d15-17 localizes to Rab7-positive intracellular structures. For this, we doubly stained *Drosophila* S2R+ cells transiently expressing HA-Tbc1d15-17,

along with Rab7-GFP or Rab5-GFP, with anti-GFP and anti-HA antibodies. The epitope-tagged Tbc1d15-17 appeared in a punctate pattern throughout the cytoplasm (Fig. 4A). Some of the Tbc1d15-17-positive puncta were also labeled for Rab7-GFP but not for Rab5-GFP (Fig. 4A), in line with the proposed role for Tbc1d15 as the GAP for Rab7.

Because Tbc1d15-17 was expected to function as a Rab7 GAP, we tested whether neuronal overexpression of constitutively active and dominant-negative Rab7 mutants (Rab7Q67L and Rab7T22N, respectively) could influence presynaptic morphology. When *UAS-rab7Q67L* was overexpressed under the control of *C155-GAL4*, we observed an increase in both bouton number and NMJ length (Figs. 3B-3D), reminiscent of defects in *tbc1d15-17* mutants. In sharp contrast, neuronal overexpression of *UAS-rab7T22N* produced the opposite effect on synaptic growth (Figs. 4B-4D). The phenotypic overlap between Rab7Q67L overexpression and *tbc1d15-17* loss-of-function supports a functional relationship between Rab7 and Tbc1d15-17 *in vivo*.

In this study, we have demonstrated a novel role for the potential Rab-GAP Tbc1d15-17 in regulating synaptic growth. Loss or neuron-specific knock-down of Tbc1d15-17 causes a phenotype of synaptic overgrowth, increasing total bouton number and NMJ length. Consistent with its proposed role as the Rab7 GAP, Tbc1d15-17 protein is able to localize to Rab7-positive intracellular structures. Indeed, genetic elevation of Rab7 activity in neurons causes an NMJ phenotype similar to that of loss-of-function *tbc1d15-17* mutants, supporting the hypothesis that Tbc1d15-17 regulates synaptic growth by inhibiting Rab7 activity. Together, our data have suggested the importance of Tbc1d15-17 and its putative substrate Rab7 in synaptic development.

Our experiments have revealed that the extent of synaptic growth is inversely correlated to Rab7 activity. At present, the mechanism of Rab7's involvement in synaptic growth regulation remains unclear. Rab7 is known to mediate the maturation of early endosomes into late endosomes and lysosomes, thereby promoting lysosomal degradation of various synaptic receptors, including the nerve growth factor Trk and the epidermal growth factor receptor (EGFR) (Ceresa and Bahr, 2006; Saxena et al., 2005). Thus, although we cannot exclude other possibilities, it is highly plausible to propose that Rab7 regulates synaptic growth by facilitating lysosomal-dependent degradation of synaptic receptors.

ACKNOWLEDGEMENTS

This work was supported by grants from the National Research Foundation of Korea (grant number 2010-0007822 to J.-H.Y. and 2011-0019228 and 2009-0071481 to S.L.).

REFERENCES

Albert, S., Will, E., and Gallwitz, D. (1999). Identification of the catalytic domains and their functionally critical arginine residues of two yeast GTPase-activating proteins specific for Ypt/Rab transport GTPases. EMBO J. *18*, 5216-5225.

Barr, F., and Lambright, D.G. (2010). Rab GEFs and GAPs. Curr. Opin. Cell Biol. *22*, 461-470.

Brand, A.H., and Perrimon, N. (1993). Targeted gene expression as a means of altering cell fates and generating dominant phenotypes. Development *118*, 401-415.

Budnik, V., Koh, Y.H., Guan, B., Hartmann, B., Hough, C., Woods, D., and Gorczyca, M. (1996). Regulation of synapse structure and function by the Drosophila tumor suppressor gene dlg. Neuron *17*, 627-640.

Ceresa, B.P., and Bahr, S.J. (2006). rab7 activity affects epidermal growth factor: epidermal growth factor receptor degradation by regulating endocytic trafficking from the late endosome. J. Biol. Chem. *281*, 1099-1106.

Jan, L.Y., and Jan, Y.N. (1982). Antibodies to horseradish peroxidase as specific neuronal markers in Drosophila and in grasshopper embryos. Proc. Natl. Acad. Sci. USA *79*, 2700-2704.

Khodosh, R., Augsburger, A., Schwarz, T.L., and Garrity, P.A. (2006). Bchs, a BEACH domain protein, antagonizes Rab11 in synapse morphogenesis and other developmental events. Development *133*, 4655-4665.

Laflamme, C., Assaker, G., Ramel, D., Dorn, J.F., She, D., Maddox, P.S., and Emery, G. (2012). Evi5 promotes collective cell migration through its Rab-GAP activity. J. Cell Biol. *198*, 57-67.

Lin, D.M., and Goodman, C.S. (1994). Ectopic and increased expression of Fasciclin II alters motoneuron growth cone guidance. Neuron *13*, 507-523.

Mori, Y., Matsui, T., Furutani, Y., Yoshihara, Y., and Fukuda, M. (2012). Small GTPase Rab17 regulates dendritic morphogenesis and postsynaptic development of hippocampal neurons. J. Biol. Chem. *287*, 8963-8973.

Nahm, M., Kim, S., Paik, S.K., Lee, M., Lee, S., Lee, Z.H., Kim, J., Lee, D., and Bae, Y.C. (2010). dCIP4 (Drosophila Cdc42-interacting protein 4) restrains synaptic growth by inhibiting the secretion of the retrograde Glass bottom boat signal. J. Neurosci. *30*, 8138-8150.

Peralta, E.R., Martin, B.C., and Edinger, A.L. (2010). Differential effects of TBC1D15 and mammalian Vps39 on Rab7 activation state, lysosomal morphology, and growth factor dependence. J. Biol. Chem. *285*, 16814-16821.

Saxena, S., Bucci, C., Weis, J., and Kruttgen, A. (2005). The small GTPase Rab7 controls the endosomal trafficking and neuritogenic signaling of the nerve growth factor receptor TrkA. J. Neurosci. *25*, 10930-10940.

Shirane, M., and Nakayama, K.I. (2006). Protrudin induces neurite formation by directional membrane trafficking. Science *314*, 818-821.

Stenmark, H. (2009). Rab GTPases as coordinators of vesicle traffic. Nat. Rev. Mol. Cell Biol. *10*, 513-525.

Stewart, B.A., Atwood, H.L., Renger, J.J., Wang, J., and Wu, C.F. (1994). Improved stability of Drosophila larval neuromuscular preparations in haemolymph-like physiological solutions. J. Comp. Physiol. A *175*, 179-191.

Wang, T., Liu, Y., Xu, X.H., Deng, C.Y., Wu, K.Y., Zhu, J., Fu, X.Q., He, M., and Luo, Z.G. (2011a). Lgl1 activation of rab10 promotes axonal membrane trafficking underlying neuronal polarization. Dev. Cell *21*, 431-444.

Wang, T., Ming, Z., Xiaochun, W., and Hong, W. (2011b). Rab7: role of its protein interaction cascades in endo-lysosomal traffic. Cell. Signal. *23*, 516-521.

Wodarz, A., Hinz, U., Engelbert, M., and Knust, E. (1995). Expression of crumbs confers apical character on plasma membrane domains of ectodermal epithelia of Drosophila. Cell *82*, 67-76.